provided the author and source are cited.

ACS AuthorChoice

Rational Re-engineering of a Transcriptional Silencing PreQ$_1$ Riboswitch

Ming-Cheng Wu,[†,‡] Phillip T. Lowe,[†,§] Christopher J. Robinson, Helen A. Vincent, Neil Dixon,[∥] James Leigh, and Jason Micklefield*

School of Chemistry and Manchester Institute of Biotechnology, The University of Manchester, 131 Princess Street, Manchester M1 7DN, United Kingdom

S *Supporting Information*

ABSTRACT: Re-engineered riboswitches that no longer respond to cellular metabolites, but that instead can be controlled by synthetic molecules, are potentially useful gene regulatory tools for use in synthetic biology and biotechnology fields. Previously, extensive genetic selection and screening approaches were employed to re-engineer a natural adenine riboswitch to create orthogonal ON-switches, enabling translational control of target gene expression in response to synthetic ligands. Here, we describe how a rational targeted approach was used to re-engineer the PreQ$_1$ riboswitch from *Bacillus subtilis* into an orthogonal OFF-switch. In this case, the evaluation of just six synthetic compounds with seven riboswitch mutants led to the identification of an orthogonal riboswitch−ligand pairing that effectively repressed the transcription of selected genes in *B. subtilis*. The streamlining of the re-engineering approach, and its extension to a second class of riboswitches, provides a methodological platform for the creation of new orthogonal regulatory components for biotechnological applications including gene functional analysis and antimicrobial target validation and screening.
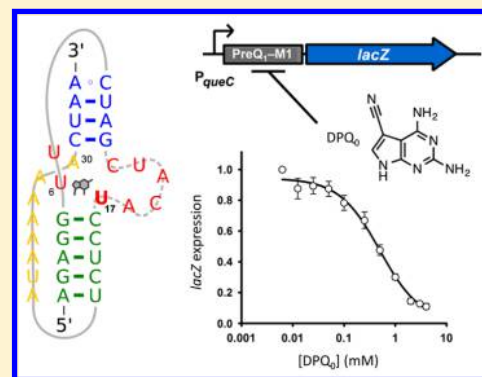
■ INTRODUCTION

Riboswitches are noncoding regions of mRNA that regulate gene expression through the selective binding of metabolites.[1,2] Most riboswitches are found within the 5′-untranslated regions (5′-UTRs) of bacterial mRNAs that encode gene products required for the biosynthesis, catabolism, or transport of the cognate metabolite.[1,2] Riboswitches exhibit a modular architecture consisting of an aptamer domain that, upon ligand binding, induces a conformational change in an overlapping expression platform, thus modulating gene expression, primarily through transcription termination or translation initiation.[1−3]

RNA-based gene regulators, such as riboswitches, are an attractive starting point for the development of new gene expression tools for the synthetic biology and biotechnology fields.[4−8] RNA regulatory components have the advantage over their protein counterparts in that they are inherently more versatile, being relatively easy to design or manipulate in a predictable manner and being transferable between organisms.[4−6] Natural riboswitches provide a diverse array of ready-made components, with different aptamer domains having been identified for more than 20 specific metabolite ligands[1,2] and expression platforms that exhibit considerable mechanistic diversity.[1,2] The modularity of these regulatory components is also demonstrated by the natural occurrence of tandem riboswitches, which can function as two-input Boolean logic gates or provide more binary switching responses.[2] Despite these advantages, most riboswitches respond to essential metabolites

that are present in cells at variable levels, and the exogenous addition of metabolites at the concentrations required to modulate riboswitch function could have adverse effects, perturbing global gene expression levels and cellular physiology.[9]

Engineered riboswitches that respond to synthetic non-natural ligands, rather than metabolites, are highly desirable.[4] The most common strategy used to create such switches is to insert RNA aptamers that have been generated by *in vitro* selection into the 5′-UTR of a target gene and to use a genetic selection or screen to isolate functioning riboswitches.[10−13] Recent studies have shown that hybrid riboswitches can also be rationally designed, through the fusion of synthetic aptamers with expression platforms derived from natural riboswitches, to create functional chimeric switches.[14,15] In theory, it should be possible to generate a riboswitch that responds to any ligand of choice using these approaches. However, there is a limited availability of synthetic aptamers that have been demonstrated to function as components of riboswitches, with only theophylline and tetracycline aptamers finding widespread use.[16] This is because the development of new aptamers *in vitro* can be laborious and, critically, does not guarantee high specificity or functionality *in vivo*.[4,17]

To address the need for new riboswitch-based gene expression tools that respond to non-natural ligands, we previously reported

a strategy for re-engineering natural riboswitches to generate orthogonal aptamer domains that are selective for artificial ligands rather than the cognate natural metabolite.[18−20] The ligand binding site of the *add* A-riboswitch from *Vibrio vulnificus* was subjected to saturation mutagenesis; then, an exhaustive chemical genetic selection strategy was used to identify functional orthogonal riboswitch−ligand combinations.[18] Through this approach, two novel mutant aptamer domains were generated that respond to triazine-based ligands.[18] Subsequent rounds of structure-guided screening identified superior second-generation pyrimidopyrimidine ligands.[20] In principle, this strategy is applicable to any riboswitch. However, the extensive selection and screening process adopted was laborious, with more than 100 potential ligands being evaluated against the panel of *add* riboswitch mutants.[18,20] With hindsight, the *add* A-aptamers could have been re-engineered through a more rational approach. Indeed, a common feature of the orthogonal aptamer−ligand pairings that we have identified is that the direction of a few key hydrogen-bonding interactions between the aptamer and ligand had been reversed, through conservative uracil to cytosine mutations, with complementary changes to the structure of the synthetic ligand. Consequently, rational redesign of natural aptamer domains should be achievable through mutations that reverse hydrogen-bond directionality, disrupting interactions between the aptamer and the natural ligand, while avoiding mutations that might adversely affect the global structure of the aptamer domain. In turn, *a priori* knowledge of the structure of the re-engineered ligand-binding pocket allows predictions to be made about the types of ligand that are likely to bind, allowing more rapid and effective screening against a smaller targeted synthetic compound library.

In this article, we demonstrate how a rational approach can be used to re-engineer the PreQ$_1$ class I riboswitch from *Bacillus subtilis*.[21−23] PreQ$_1$ class I riboswitches, commonly found in Firmicutes and Proteobacteria,[21,24] regulate genes required for the biosynthesis of the hypermodified nucleotide queuosine, present at the wobble position of GUN tRNAs.[21,25] The minimal PreQ$_1$ aptamer domain is the smallest known riboswitch aptamer, at just 34 nucleotides in length (Figure 1A), and is selective for queuosine precursors 7-aminomethyl-7-deazaguanine (PreQ$_1$) and 7-cyano-7-deazaguanine (PreQ$_0$).[21] Ligand binding stabilizes a H-type pseudoknot in the aptamer domain (Figure 1B),[22,23] which leads to the formation of a downstream transcriptional terminator stem required to repress gene expression (Figure S1).[21] We introduced mutations at three key sites in the ligand-binding pocket to disrupt hydrogen bonding to the natural queuosine precursors, and these candidate aptamers were evaluated *in vivo* against a small rationally designed library of synthetic compounds. From this approach, a functional mutant riboswitch−ligand pairing was identified that was highly effective in repressing gene expression in *B. subtilis*.

RESULTS AND DISCUSSION

Targeted Mutagenesis of the PreQ$_1$ Riboswitch. The PreQ$_1$ class I riboswitch from *B. subtilis* was considered to be a good candidate for re-engineering, as it is well-characterized and analogues of the natural ligands are both synthetically accessible and likely to be cell-permeable. From published structures of the PreQ$_1$ aptamer, it is apparent that Watson−Crick base pairing between the conserved cytidine C17 residue and PreQ$_1$ is essential in ligand recognition.[22,23] This canonical base pair interaction, along with a *trans* sugar edge/Watson−Crick base pairing with A30 and additional hydrogen bonding to G5 and U6,

allows for complete recognition of the PreQ$_1$ ligand by the riboswitch aptamer (Figure 1B,C). On the basis of these
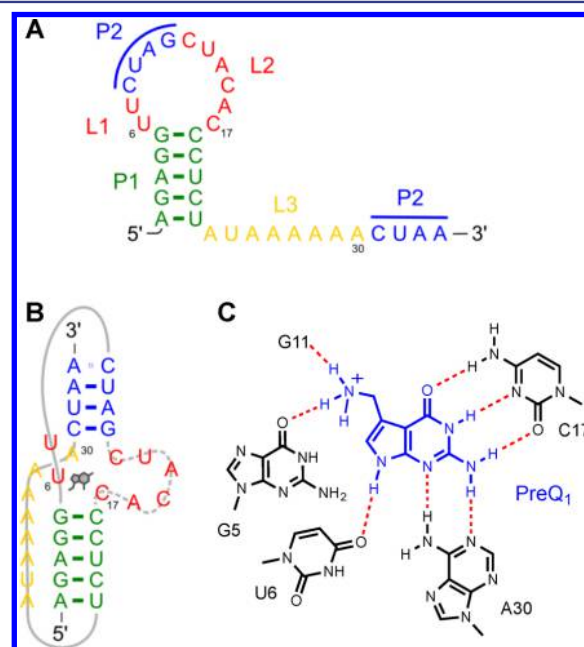

Figure 1. Secondary structure of the PreQ$_1$-I aptamer and H-bond ligand contacts. (A) Stems P1 (green) and P2 (blue) are connected through three loop regions (L1−L3). (B) Stem P2 is formed through a tertiary interaction, which is stabilized by ligand binding, resulting in a H-type pseudoknot. (C) The PreQ$_1$ ligand (blue) H-bonds with one residue from each of the three loops, U6 (L1), C17 (L2), and A30 (L3). This ligand-binding core is stacked between the two stems of the aptamer, with the aminomethyl group of PreQ$_1$ pointing out into the major groove, where it interacts with G5 (P1) and the phosphate of G11 (P2). (See Figure S1 for more details.)

structural insights, residues G5, U6, and C17, along with residue C18 which Watson−Crick pairs with G5 in the P1 stem, were subjected to site-directed mutagenesis to alter the binding specificity of the aptamer toward new non-native ligands. A30 was not considered for mutagenesis, as it H-bonds to the C2-amino group of the ligand. The C2-amino group was shown to be essential for ligand binding by the PreQ$_1$ riboswitch[21] and would be required for H-bonding to either C17 or U17. To avoid unnecessarily perturbing riboswitch folding, while keeping the dimensions of the ligand-binding pocket constant, the transversion of pyrimidines to purines or *vice versa* was avoided, resulting in a library of just seven mutants: the M1 (C17U), M2 (U6C), and M3 (G5A) single mutants; M4 (G5A, C18U) and M5 (U6C, C17U) double mutants; M6 (G5A, C17U, C18U) triple mutant; and M7 (G5A, U6C, C17U, C18U) quadruple mutant.

It was anticipated that riboswitches possessing the C17U mutation might recognize synthetic diamino-faced compounds (Figure 2, **1−6**). Similarly, U6C was envisaged to potentially alter riboswitch specificity from the native deazapurine ligands to furopyrimidines (**3−6**), whereas G5A might permit interactions with compounds possessing different C7 side chains (**1** and **4−6**). Given that the G5A mutation was predicted to disrupt formation of the P1 aptamer stem, the complementary C18U was also included alongside G5A (see Figure S1 for further information). The selected mutations were introduced into a *lacZ* expression vector, in which the promoter and entire 5′-UTR
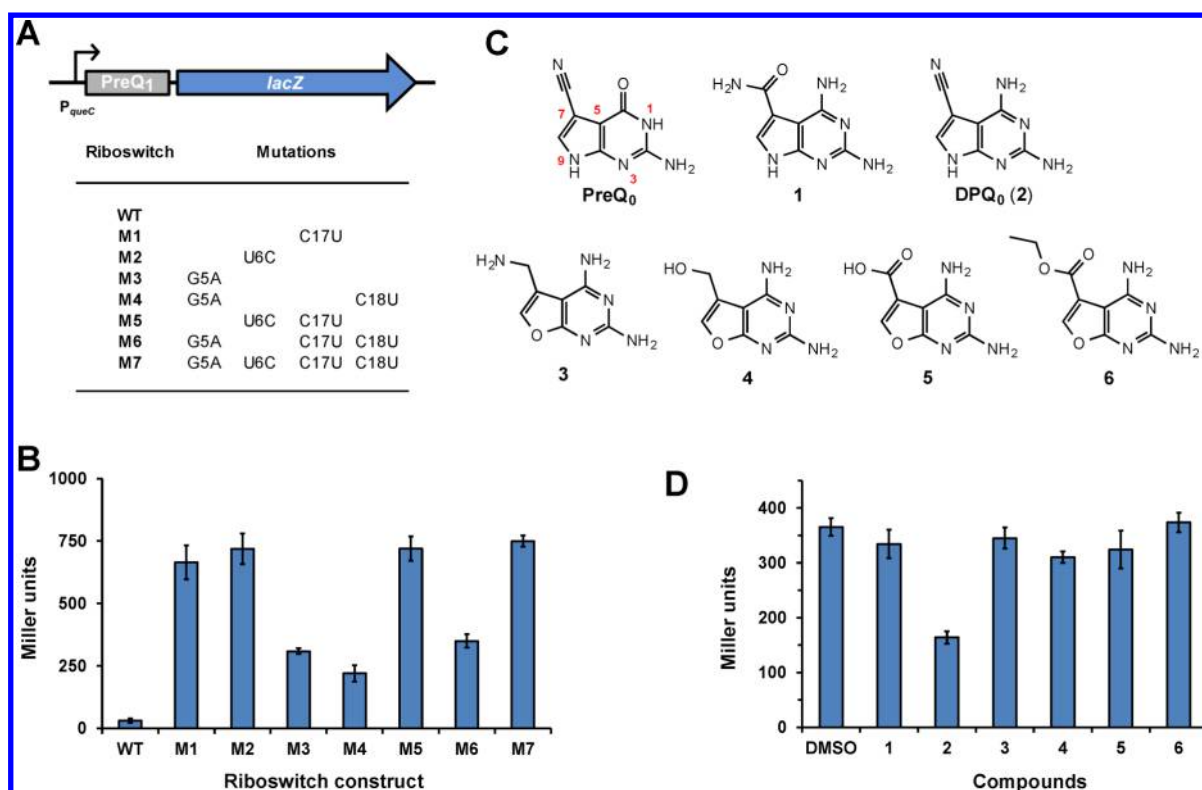
Figure 2. Screening PreQ$_1$ riboswitch mutants for control of LacZ expression in *B. subtilis*. (A) Schematic of the chromosomally integrated LacZ expression construct. The *lacZ* gene (blue box arrow) is transcribed from the *B. subtilis queCDEF* constitutive promoter (black line arrow). A wild-type or mutant PreQ$_1$ riboswitch (gray box) terminates transcription upon ligand binding. Riboswitch mutations tested in this study are tabulated. (B) β-Galactosidase activity of wild-type and mutant riboswitch constructs assayed in the absence of exogenous ligand. (C) Structures of synthetic compounds screened for activity with mutant riboswitch constructs. (D) β-Galactosidase activity of the M1 (C17U) riboswitch construct assayed in the presence of 1 mM of the compounds above. Data represent the mean of three repeats, with error bars indicating standard deviation.

of the *queCDEF* operon, encompassing the PreQ$_1$ riboswitch aptamer domain and expression platform, controlled expression of the *lacZ* gene (Figures 2A and S2A).[21] The constructs were then integrated into the chromosome of *B. subtilis* to generate reporter strains enabling riboswitch–ligand interactions to be monitored *in vivo* using a modified Miller assay.[26]

In Vivo Functionality of PreQ$_1$ Riboswitch Mutants. Levels of β-galactosidase (LacZ) activity were determined initially in the absence of ligand (Figure 2B). The strain possessing the wild-type riboswitch produced very low basal levels of LacZ activity, suggesting that cellular levels of PreQ$_1$ and PreQ$_0$ were sufficient to bind the wild-type riboswitch and repress LacZ expression; this demonstrates how the parent riboswitch is of little utility as a regulatory tool in cells that produce the natural ligands. In contrast, all of the mutant riboswitch strains exhibited elevated levels of LacZ activity, presumably because they no longer bind the native ligands or because they have lost the ability to function as transcriptional terminating elements. Subsequently, transformants were screened for their ability to control LacZ expression in response to the exogenous addition of PreQ$_0$. The LacZ activity of all mutant riboswitch transformants was unaffected by the addition of exogenous PreQ$_0$ (at 2.5 mM), demonstrating that these mutants no longer respond to PreQ$_0$ (Figure S3A). The Breaker group previously reported structural modulation of a C17U mutant of the PreQ$_1$ riboswitch in the presence of 2,6-diaminopurine (DAP).[21] Therefore, we also tested DAP in our assay, but no significant repression of LacZ activity was observed for any of our mutant PreQ$_1$ riboswitches in the presence of 2.5

mM DAP (Figure S3B). This demonstrates that while DAP may bind to the M1 (C17U) aptamer *in vitro* it is not capable of controlling gene expression *in vivo* through the M1 riboswitch, so it is not a suitable orthogonal riboswitch ligand.

The mutant strains fell into two distinct groups: those that exhibited high levels of LacZ expression in the absence of ligand (M1, M2, M5, and M7) and those that exhibited moderate levels of LacZ expression (M3, M4, and M6). It was noted that the moderate LacZ expressors all contained the G5A mutation, which is situated underneath the ligand-binding pocket at the top of the P1 stem. It is possible that this mutation leads to alternative folding of the riboswitch, interfering with downstream transcription (reducing LacZ expression). The compensatory C18U mutation was designed to restore P1 stem integrity by allowing base pairing to the G5A mutation; however, mutants M4 and M6 produced only intermediate levels of LacZ despite having both mutations present. These data suggest that the G5A mutation is unsuitable for the development of orthogonally selective PreQ$_1$ riboswitches. In light of this, the single mutant M1 (C17U) and double mutant M5 (U6C, C17U) were considered to be the best candidates for the creation of orthogonally selective riboswitches and were therefore prioritized for further study.

In Vivo Evaluation of Candidate Ligands. Six potential ligand compounds **1**−**6** (Figure 2C) were designed and synthesized, focusing on diamino-faced analogues of PreQ$_1$ and PreQ$_0$, to target the C17U mutation present in both the M1 and M5 riboswitches. In addition, four of these compounds were synthesized with an oxygen at position 9 to accommodate the U6C mutation in M5. This targeted compound library was

screened for the ability to repress LacZ activity controlled by mutant riboswitches M1 (Figure 2D) and M5 (Figure S4A). This strategy identified a functional riboswitch—ligand pairing between the M1 mutant and ligand **2**, the diamino analogue of $PreQ_0$ (DPQ_0). The M1 riboswitch exhibited selectivity, mediating *in vivo* repression only in the presence of DPQ_0 (**2**), despite all library compounds having a diamino-face. Furthermore, when tested against other riboswitch mutants that contain the C17U mutation (M1, M5, M6, and M7), DPQ_0 was active only against M1 (Figure S3C). The M1—DPQ_0 pairing was capable of dose-dependent control of *lacZ* expression, with an IC_{50} value of 498 μM and ~90% repression observed at DPQ_0 concentrations of 2 mM or higher (Figure 3A). The proposed
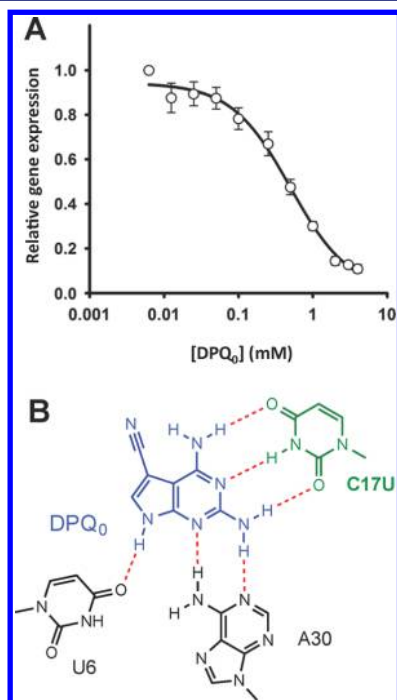

Figure 3. Dose-dependent repression of gene expression using the orthogonal M1 riboswitch. (A) *B. subtilis* cells with *lacZ* under transcriptional control of the M1 riboswitch were assayed for β-galactosidase activity with DPQ_0 (6.25 μM to 4 mM). Data represent the mean of three repeats, with error bars indicating standard deviation. The data were fit with a four-parameter logistic function to derive an IC_{50} of 498 μM. (B) Proposed H-bonding model for DPQ_0 (blue) binding to the M1 riboswitch. The mutated C17U residue is shown in green. H-bonds are depicted as red dashed lines.

binding model of M1 bound to DPQ_0 (Figure 3B) shows how the C17U mutation alters the base pairing complementarity from the guanine-face of $PreQ_0$ to the diamino-face of its analogue, DPQ_0. Since $PreQ_0$ cannot repress the M1 riboswitch (Figure S3A), this mutant riboswitch is orthogonal with respect to the wild-type system in terms of *in vivo* functionality. Growth rate studies (Figure S5) also reveal that DPQ_0 is not toxic to *B. subtilis* at concentrations required to modulate M1 riboswitch activity.

The U6C mutation was rationalized to switch the specificity of the riboswitch, from deazapurines, which possess an N9 hydrogen-bond donor, to synthetic furopyrimidines with an O9 H-bond acceptor. Accordingly, several diamino-faced ligands were synthesized with an oxygen at position 9 (**3**−**6**); however, none of them were capable of repressing the M5 (U6C, C17U) riboswitch under the conditions of our LacZ assay (Figure S4A).

The U6 residue also plays a role in $PreQ_1$ riboswitch folding, as it base pairs with the Hoogsteen edge of A29.[22,23] This base pair will be lost with the U6C mutation, which may disrupt aptamer folding and ligand-binding kinetics. We therefore investigated whether the M5 riboswitch could repress LacZ expression when cells were grown at 16 °C, rather than at 37 °C (Figure S4B). Under these conditions, ligand **3** was capable of modestly repressing LacZ expression through the M5 riboswitch (28% at 2 mM), suggesting that lower temperatures stabilize the ligand-bound pseudoknot and/or alter kinetics of transcription to allow the riboswitch to function. Surprisingly, **3** was found to repress LacZ expression under the control of the M1 riboswitch to an even greater extent (59% at 2 mM), despite there being a predicted lone pair clash between U6 and O9 of ligand **3**. These observations suggest that there may be some flexibility in the positioning of U6 to accommodate mismatches in H-bonding potential, which, when combined with the structural disruption resulting from mutation of this residue, indicate that U6 is not a suitable target residue for creating robustly functioning orthogonal riboswitch mutants.

***In Vitro* Characterization of DPQ_0 Binding to the Orthogonal M1 Riboswitch Aptamer.** $PreQ_0$ is converted directly into $PreQ_1$ by the NADPH-dependent enzyme QueF,[27] which reduces the nitrile group to an aminomethyl moiety. Since DPQ_0 is a diamino-faced analogue of $PreQ_0$, the possibility that QueF might reduce the nitrile group of DPQ_0 *in vivo* was investigated. The nitrile reductase QueF from *B. subtilis* was overproduced in *Escherichia coli* by standard protocols. Although recombinant QueF was shown to reduce $PreQ_0$ *in vitro* (Figure S6), it did not accept DPQ_0 as an alternative substrate. This suggests that DPQ_0, and not its reduced aminomethyl derivative, acts directly on the M1 riboswitch to control gene expression in *Bacillus*.

To further confirm that DPQ_0 is the *in vivo* ligand for the M1 riboswitch, we used isothermal titration calorimetry (ITC) to study the binding of DPQ_0 and $PreQ_0$ to *in vitro* transcribed M1 and wild-type aptamer domains. The native $PreQ_0$ ligand was found to bind to the wild-type 34 nt minimal aptamer domain with an apparent equilibrium dissociation constant (K_D) of 0.57 ± 0.02 μM (Figure 4A,C). This value was larger than the 0.1 μM K_D reported from in-line probing analysis of $PreQ_0$ binding to a 52 nt fragment of the *B. subtilis* $PreQ_1$ riboswitch.[21] However, this fragment included an additional stem loop structure (P0) at the 5′-end of the minimal aptamer domain, which was reported to increase affinity of the aptamer for the natural ligand.[21] Therefore, the apparent K_D we report here for $PreQ_0$ binding to the minimal 34 nt aptamer is consistent with the modest decrease in binding affinity observed when the P0 stem is absent. The synthetic ligand DPQ_0 was found to bind the mutant M1 aptamer with an apparent K_D of 14.6 ± 1.46 μM (Figure 4B,C), 26-fold higher than that of the wild-type aptamer—$PreQ_0$ pairing. This reduction in binding affinity might be attributed to perturbation of the structure or folding of the aptamer—ligand complex as a result of the mutation of a key residue (C17U) and its binding to a synthetic ligand analogue. Importantly, *in vitro* orthogonality was observed between the two aptamer—ligand pairings, as $PreQ_0$ was shown to have no affinity for the mutant M1 aptamer and, similarly, DPQ_0 had no affinity for the wild-type $PreQ_1$ aptamer.

It was apparent from the ITC analysis that the predicted stoichiometry of $PreQ_0$ binding to the wild-type aptamer was too low (Figure 4C). An *n* value of 0.27 suggests that only around one-quarter of the aptamer sample was ligand-binding
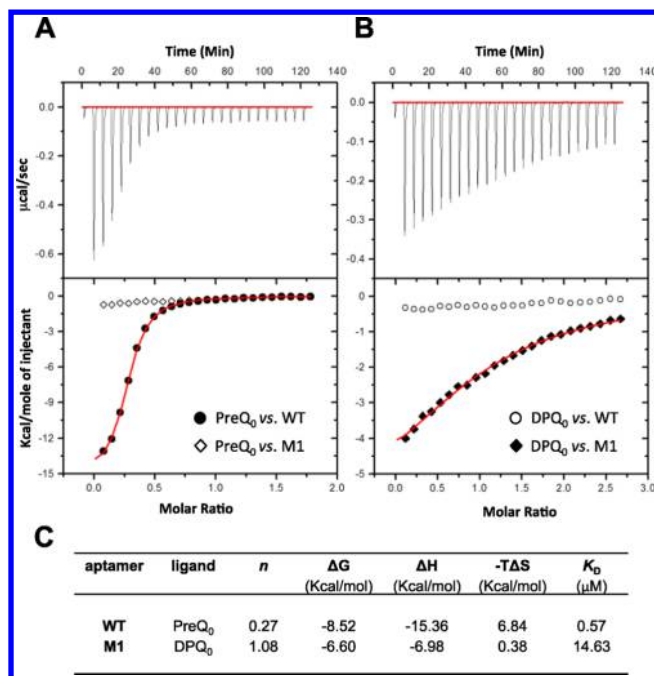
Figure 4. ITC analysis of aptamer−ligand interactions. (A) Upper panel: wild-type PreQ$_1$ aptamer titrated with PreQ$_0$. Lower panel: binding isotherms for 18.7 μM wild-type (black circles) or mutant M1 (white diamonds) aptamers titrated with 150 μM PreQ$_0$. (B) Upper panel: mutant M1 aptamer titrated with DPQ$_0$. Lower panel: binding isotherms for 18.7 μM mutant M1 (black diamonds) or wild-type (white circles) aptamers titrated with 225 μM DPQ$_0$. Experiments were conducted at 25 °C in 50 mM HEPES (pH 7.5) buffer containing 100 mM KCl and 20 mM MgCl$_2$. (C) Curves were fitted in Origin, using the supplied software (MicroCal), to calculate the thermodynamic parameters presented.
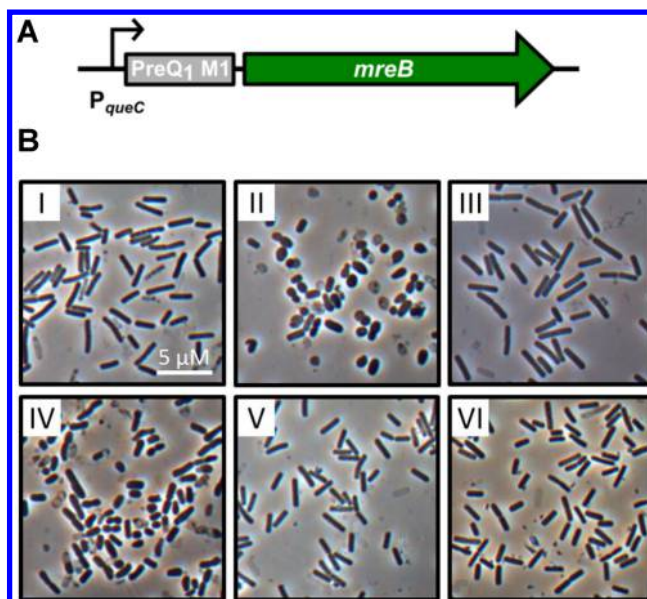

Figure 5. Controlling cell morphology using the orthogonal M1 riboswitch. (A) The MreB expression construct. The *mreB* gene (green arrow) is transcribed from the *B. subtilis queCDEF* constitutive promoter (black arrow). The M1 riboswitch (gray box) terminates transcription upon binding DPQ$_0$. (B) Conditional gene repression affects *B. subtilis* morphology. The MreB expression construct was chromosomally integrated into an *mreB* knockout strain of *B. subtilis* (Δ*mreB*) to create the repressible M1-*mreB* strain. Cells were imaged at 60× magnification: (I) wild-type, (II) Δ*mreB* cells, (III) M1-*mreB* cells, (IV) M1-*mreB* cells with 2 mM DPQ$_0$, (V) wild-type cells with 2 mM DPQ$_0$, and (VI) M1-*mreB* cells with 2 mM PreQ$_0$. For further images, see Figure S8, Supporting Information.

competent. We suspected that this was a consequence of a previously reported PreQ$_1$ aptamer dimerization artifact.[28,29] We prepared aptamer samples incorporating the C12U mutation to prevent dimerization without disrupting important interactions in the aptamer−ligand complex.[22,23] Although the C12U mutation prevented aptamer dimerization, it reduced the affinity of the wild-type aptamer for PreQ$_0$ (K_D of 1.92 ± 0.08 μM) and led to a lack of detectable binding between DPQ$_0$ and the C12U mutant of M1 (Figure S7). It should be noted that dimerization of aptamers affects only the *n* parameter during ITC analysis; all other parameter calculations are dependent solely on an accurate determination of the ligand concentration in the syringe.[30] Therefore, apparent K_D estimates presented here are nonetheless reliable (Figure 4C).

Regulation of MreB Expression Demonstrates M1 Utility. MreB is an actin homologue that plays a crucial role in maintaining the distinctive rod-shaped morphology of *B. subtilis* and many other bacterial species and is a promising target for antimicrobial drug screening.[31] To demonstrate the potential applications of our M1−DPQ$_0$ riboswitch−ligand pairing in controlling native gene expression, we created a strain of *B. subtilis* in which the expression of MreB was placed under the conditional control of the full-length M1 riboswitch (Figure 5A).

Wild-type *B. subtilis*, which can freely express MreB, adopts a rod-shaped morphology (Figure 5B-I).[32] An *mreB* deletion strain of *B. subtilis* (Δ*mreB*) exhibits compromised growth, with cells round and swollen in shape (Figure 5B-II). A linear M1-*mreB* construct was chromosomally integrated into Δ*mreB* cells at the

amyE locus to produce the repressible M1-*mreB* strain. In the absence of ligand, MreB is expressed by the M1-*mreB* strain to restore the rod-shaped morphology (Figure 5B-III), demonstrating that the integrated construct successfully complements the Δ*mreB* phenotype. Following supplementation of the cell media with DPQ$_0$, M1 repressed expression of MreB in the M1-*mreB* strain (Figure 5B-IV). *In vivo* orthogonality was demonstrated, as the same concentration of PreQ$_0$ had no morphological effect on M1-*mreB* cells (Figure 5B-VI). Similarly, the morphology of the wild-type strain was unaffected by the addition of DPQ$_0$ (Figure 5B-V), confirming that the effects of this ligand on M1-*mreB* cells are mediated through the M1 riboswitch.

Measurement of *B. subtilis* cell dimensions (Figure S9) revealed that while the addition DPQ$_0$ had a significant effect ($P < 0.001$) on the M1-*mreB* strain, reducing the mean length/width ratio of cells from 3.64 to 1.74, it had little effect on wild-type cells (5.39 and 5.19 in the absence and presence of DPQ$_0$, respectively). These data indicate that DPQ$_0$ affects the morphology of M1-*mreB* cells by repressing *mreB* expression through its specific interaction with the M1 riboswitch. Furthermore, western blotting revealed that MreB protein levels were significantly reduced in the M1-*mreB* strain following incubation with DPQ$_0$ (Figure S10). These studies show how the orthogonal M1−DPQ$_0$ riboswitch−ligand pairing can be used to regulate the expression of native genes in *B. subtilis*, to complement knockout phenotypes, for gene functional analysis, and for other purposes.

■ CONCLUSIONS

Natural riboswitch aptamer domains and expression platforms represent a diverse toolbox of modular gene regulatory components. However, if this resource is to be fully exploited in the creation of new genetic circuits, there is a need to develop riboswitch aptamers that are orthogonal to one another and that respond to synthetic or non-native ligands. Previous efforts to develop synthetic aptamers or to re-engineer natural aptamers have involved extensive *in vitro* selection[4,17] or laborious screening procedures.[18,20] In this article, we demonstrate how a more rational targeted approach can be used to streamline the process of creating orthogonal riboswitch tools.

On the basis of previous biochemical and structural studies,[21−23] just seven variants of the PreQ$_1$-I riboswitch and six synthetic ligand candidates were designed and tested for their ability to repress gene expression. A single mutant (C17U) M1, which does not respond to the natural ligand PreQ$_0$, was shown to provide effective dose-dependent repression of *lacZ* expression in *B. subtilis* upon addition of a diamino analogue DPQ$_0$. ITC experiments revealed that M1 binds DPQ$_0$, but has no affinity for PreQ$_0$, and conversely that the wild-type aptamer binds PreQ$_0$, but not DPQ$_0$. Interestingly, 2,6-diaminopurine (DAP), which had previously been shown to bind to M1 *in vitro*,[21] was unable to modulate M1-*lacZ* expression *in vivo*. The *in vivo* selectivity for DPQ$_0$ over DAP may be due to differences in the rates of ligand−riboswitch association.[21] Similar kinetic selectivity is suggested to account for how the PreQ$_1$ riboswitch discriminates between PreQ$_1$ and guanine *in vivo*, despite binding both ligands *in vitro*.[21] In addition, M1 and a double mutant (U6C, C17U), M5, designed to recognize furopyrimidine analogues, afforded repression of *lacZ* expression with furopyrimidine 3, but they did so only when cells were grown at lower temperature (16 °C). The riboswitch−furopyrimidine complexes may be unstable at higher temperatures, or, alternatively, the kinetics of riboswitch ligand binding and transcription may be less favorable.

To demonstrate the general applicability of the orthogonal M1−DPQ$_0$ riboswitch, we created conditional mutants of the bacterial actin homologue MreB in *B. subtilis*, enabling cell morphology to be controlled through the exogenous supply of DPQ$_0$. MreB is essential for the normal growth of rod-shaped bacteria and has been identified as a potential antibiotic target.[31] The dose-dependent control of *mreB* expression levels could provide, therefore, a useful tool in creating sensitive strains for antibiotic screening. Establishing tunable conditional mutants of essential genes in pathogenic strains is important in antimicrobial target validation and whole cell screening;[33−35] by lowering the levels of essential gene products in the cell, it is possible to develop more sensitive screens for compounds that selectively inhibit their function. Many important pathogenic and antibiotic-resistant bacteria contain native PreQ$_1$ riboswitches, including Firmicutes (e.g., *Staphylococcus, Clostridium, Listeria, Enterococcus*) and Proteobacteria (e.g., *Campylobacter, Salmonella, Neisseria*).[24] M1 variants of the native PreQ$_1$ riboswitches might be deployed, therefore, as host-optimized expression tools for antibiotic screening and target validation purposes in these pathogenic strains. Such tools would be timely given the problems of antimicrobial resistance and the lack of alternative tunable expression systems for interrogating many microbial pathogens.

■ MATERIALS AND METHODS

Ligand Synthesis. Pyrrolo[2,3-*d*]pyrimidines (PreQ$_0$, **1** and **2**) and furo[2,3-*d*]pyrimidines (**3-6**) were prepared in one or two synthetic steps from the inexpensive precursors, 2,4,6-triaminopyrimidine or 2,4-diamino-6-hydroxypyr-imidine (Sigma-Aldrich), following established procedures (see the Supporting Information for full details).

Construction of the Riboswitch-Controlled LacZ Expression Constructs. The pDG1661 vector[36] containing the native promoter and the entire PreQ$_1$ riboswitch, amplified from the upstream region of *B. subtilis queCDEF* operon (Figure S2A), was kindly supplied by the Breaker lab.[21] To generate riboswitch mutants, two flanking master primers (MC4 and MC5) and two internal mutagenic primers (MC6 to MC19) were designed to amplify 5′ and 3′ fragments of the PreQ$_1$ riboswitch (Table S1). Overlapping PCR was then employed to join both fragments together, generating the complete mutant PreQ$_1$ riboswitch sequences, which were cloned into the *Eco*RI and *Bam*HI sites of pDG1661, upstream of the *lacZ* reporter gene. The resulting plasmids were verified by sequencing and transformed into *B. subtilis* 1A40, where they integrated into the *amyE* locus of the chromosome by homologous recombination.[21]

***β*-Galactosidase (LacZ Expression) Assays.** A high-throughput microplate method for quantifying *β*-galactosidase activity in *B. subtilis* was modified from that described in Lynch et al.[26] Overnight cultures were diluted 50-fold into 190 μL of nutrient broth, containing 5 μg/mL chloramphenicol and either 10 μL of ligand in DMSO or with DMSO alone, and were then left to grow in a 96-well plate at 37 °C. A microplate reader (Anthos Zenyth 3100) was used to monitor OD$_{595}$ until it reached the 0.085−0.14 range (equivalent to an OD$_{595}$ of 0.3−0.5 in a 1 cm path length cuvette); cells were then lysed by the addition of 20 μL PopCulture reagent (Novagen), containing 40 U/mL lysozyme. Lysed cultures were diluted 10-fold into 150 μL of Z buffer (60 mM Na$_2$HPO$_4$, 40 mM NaH$_2$PO$_4$, 10 mM KCl, 1 mM MgSO$_4$, 50 mM *β*-mercaptoethanol, pH 7.0). The *β*-galactosidase reaction was started by adding 30 μL of *O*-nitrophenyl-*β*-D-galactoside (4 mg/mL in Z buffer), incubated at 30 °C until a yellow color developed, and then quenched by adding 75 μL of 1 M Na$_2$CO$_3$. The length of time between substrate addition and quenching and the OD$_{405}$ were recorded. The Miller units were calculated using the following formula: Miller units = $1000 \times \{OD_{405}/(OD_{595} \times time \times [volume\ of\ cell\ lysate/total\ volume])\}$

Preparation of RNA Aptamers and Isothermal Titration Calorimetry. Riboswitch aptamers were prepared by *in vitro* transcription following a protocol modified from Gurevitch.[37] Briefly, dsDNA templates (comprising the aptamer sequence downstream of the T7 RNA polymerase promoter) were created by annealing complementary primers purchased from Sigma-Aldrich (Table S1). Transcription reactions were performed by incubating T7 RNA polymerase with dsDNA templates and 6 mM each of ATP, UTP, GTP, CTP, in 30 mM Tris buffer (pH 8.0), 28 mM MgCl$_2$, 20 mM DTT, 3.4 mM spermidine, and 0.01% Triton X-100, for 4 h at 37 °C. Transcription reactions were resolved by 12% PAGE under denaturing conditions (8 M urea), with bands excised and RNA recovered by the crush-and-soak method. Aptamers were then dialyzed overnight at 4 °C into ITC buffer: 50 mM HEPES (pH 7.5), 100 mM KCl, 20 mM MgCl$_2$. Ligand solutions were prepared in the same buffer following dialysis. Samples were degassed, and ITC experiments were performed at 25 °C using a VP-ITC microcalorimeter (Microcal Inc.). Experiments were conducted with the RNA aptamer sample in the cell, titrated with one 2 μL injection and then twenty-four 12 μL injections of ligand solution.

Construction of the M1 Riboswitch-Controlled *mreB* Expression Construct. The *mreB* gene was amplified from *B. subtilis* 168 by primers MC20 and MC21 (Table S1) and cloned into the *Eco*RI and *Bam*HI sites of pDG1662. A sequence composed of the *amyE*-front fragment and *mreB* gene was amplified using primers MC22, MC23, MC24, and MC25. Separately, another sequence composed of the M1-riboswitch mutant, the *cat* (chloramphenicol resistance) gene, and the *amyE*-back fragment was amplified from the corresponding LacZ expression construct in pDG1661 (see above) using primers MC26, MC27, MC28, and MC29. The two sequences were spliced together through an identical 50 bp linker region by overlapping PCR to generate a linear construct with flanking *amyE*-front and *amyE*-back sequences

for homologous recombination (Figure S2B). This linear DNA construct was transformed into *B. subtilis* 3725 cells and integrated into the *amyE* locus. Cell morphology (MreB expression) assays were carried out as described previously[20] (see the Supporting Information for further details).

■ ASSOCIATED CONTENT

Ⓢ Supporting Information

Further experimental information; details of ligand synthesis and characterization. Figure S1: Mechanism and mutagenesis of the PreQ$_1$ class I riboswitch from the *queCDEF* operon of *B. subtilis*. Figure S2: Construction of the LacZ and MreB expression constructs. Figure S3: Screening PreQ$_1$ riboswitch mutants for control of LacZ expression. Figure S4: Screening for compounds which repress the PreQ$_1$ riboswitch mutant M5. Figure S5: Effects of DPQ$_0$ on the growth of *B. subtilis*. Figure S6: QueF nitrile reductase assay. Figure S7: Analysis of PreQ$_1$ aptamers mutated to prevent dimerization. Figure S8: Additional microscopy images of *B. subtilis* cells used in the MreB study. Figure S9: Cellular dimensions measured for various *B. subtilis* strains in the presence or absence of the indicated compounds. Figure S10: Analysis of MreB protein expression. Table S1: Primers used in this study. The Supporting Information is available free of charge on the ACS Publications website at DOI: 10.1021/jacs.5b03405.

■ AUTHOR INFORMATION

Corresponding Author
*jason.micklefield@manchester.ac.uk

Present Addresses
‡(M.-C.W.) Department of Entomology, National Chung Hsing University, Taichung, Taiwan.
§(P.T.L) School of Chemistry, University of St Andrews, St Andrews KY16 9ST, United Kingdom.
∥(N.D.) Faculty of Life Sciences, University of Manchester, Manchester M13 9PL, United Kingdom.

Author Contributions
†M.-C.W. and P.T.L. contributed equally to this work.

Notes
The authors declare no competing financial interest.

■ ACKNOWLEDGMENTS

■ REFERENCES

(1) Serganov, A.; Nudler, E. *Cell* **2013**, *152*, 17−24.
(2) Breaker, R. R. *Cold Spring Harbor Perspect. Biol.* **2012**, *4*, No. a003566.
(3) Garst, A. D.; Edwards, A. L.; Batey, R. T. *Cold Spring Harbor Perspect. Biol.* **2011**, *3*, No. a03533.
(4) Link, K. H.; Breaker, R. R. *Gene Ther.* **2009**, *16*, 1189−1201.
(5) Chappell, J.; Takahashi, M. K.; Meyer, S.; Loughrey, D.; Watters, K. E.; Lucks, J. B. *Biotechnol. J.* **2013**, *8*, 1379−1395.
(6) Vazquez-Anderson, J.; Contreras, L. M. *RNA Biol.* **2013**, *10*, 1778−1797.
(7) Berens, C.; Groher, F.; Suess, B. *Biotechnol. J.* **2015**, *10*, 246−257.
(8) Berens, C.; Suess, B. *Curr. Opin. Biotechnol.* **2015**, *31*, 10−15.
(9) Cho, B. K.; Federowicz, S. A.; Embree, M.; Park, Y. S.; Kim, D.; Palsson, B.Ø. *Nucleic Acids Res.* **2011**, *39*, 6456−6464.
(10) Weigand, J. E.; Sanchez, M.; Gunnesch, E. B.; Zeiher, S.; Schroeder, R.; Suess, B. *RNA* **2007**, *14*, 89−97.
(11) Sharma, V.; Nomura, Y.; Yokobayashi, Y. *J. Am. Chem. Soc.* **2008**, *130*, 16310−16315.
(12) Fowler, C. C.; Brown, E. D.; Li, Y. *ChemBioChem* **2008**, *9*, 1906−1911.
(13) Lynch, S. A.; Gallivan, J. P. *Nucleic Acids Res.* **2009**, *37*, 184−192.
(14) Ceres, P.; Garst, A. D.; Marcano-Velázquez, J. G.; Batey, R. T. *ACS Synth. Biol.* **2013**, *2*, 463−472.
(15) Ceres, P.; Trausch, J. J.; Batey, R. T. *Nucleic Acids Res.* **2013**, *41*, 10449−10461.
(16) Groher, F.; Suess, B. *Biochim. Biophys. Acta, Gene Regul. Mech.* **2014**, *1839*, 964−973.
(17) Wittmann, A.; Suess, B. *FEBS Lett.* **2012**, *586*, 2076−2083.
(18) Dixon, N.; Duncan, J. N.; Geerlings, T.; Dunstan, M. S.; McCarthy, J. E.; Leys, D.; Micklefield, J. *Proc. Natl. Acad. Sci. U. S. A.* **2010**, *107*, 2830−2835.
(19) Dixon, N.; Robinson, C. J.; Geerlings, T.; Duncan, J. N.; Drummond, S. P.; Micklefield, J. *Angew. Chem., Int. Ed.* **2012**, *51*, 3620−3624.
(20) Robinson, C. J.; Vincent, H. A.; Wu, M.-C.; Lowe, P. T.; Dunstan, M. S.; Leys, D.; Micklefield, J. *J. Am. Chem. Soc.* **2014**, *136*, 10615−10624.
(21) Roth, A.; Winkler, W. C.; Regulski, E. E.; Lee, B. W.; Lim, J.; Jona, I.; Barrick, J. E.; Ritwik, A.; Kim, J. N.; Welz, R.; Iwata-Reuyl, D.; Breaker, R. R. *Nat. Struct. Mol. Biol.* **2007**, *14*, 308−317.
(22) Klein, D. J.; Edwards, T. E.; Ferré-D'Amaré, A. R. *Nat. Struct. Mol. Biol.* **2009**, *16*, 343−344.
(23) Kang, M.; Peterson, R.; Feigon, J. *Mol. Cell* **2009**, *33*, 784−790.
(24) McCown, P. J.; Liang, J. J.; Weinberg, Z.; Breaker, R. R. *Chem. Biol.* **2014**, *21*, 880−889.
(25) Iwata-Reuyl, D. *Bioorg. Chem.* **2003**, *31*, 24−43.
(26) Lynch, S. A.; Desai, S. K.; Sajja, H. K.; Gallivan, J. P. *Chem. Biol.* **2007**, *14*, 173−184.
(27) Reader, J. S.; Metzgar, D.; Schimmel, P.; de Crécy-Lagard, V. *J. Biol. Chem.* **2003**, *279*, 6280−6285.
(28) Rieder, U.; Kreutz, C.; Micura, R. *Proc. Natl. Acad. Sci. U. S. A.* **2010**, *107*, 10804−10809.
(29) Eichhorn, C. D.; Feng, J.; Suddala, K. C.; Walter, N. G. *Nucleic Acids Res.* **2012**, *40*, 1345−1355.
(30) Tellinghuisen, J.; Chodera, J. D. *Anal. Biochem.* **2011**, *414*, 297−299.
(31) Bean, G. J.; Flickinger, S. T.; Westler, W. M.; McCully, M. E.; Sept, D.; Weibel, D. B.; Amann, K. J. *Biochemistry* **2009**, *48*, 4852−4857.
(32) Formstone, A.; Errington, J. *Mol. Microbiol.* **2005**, *55*, 1646−1657.
(33) Abrahams, G. L.; Kumar, A.; Savvi, S.; Hung, A. W.; Wen, S.; Abell, C.; Barry, C. E., III; Sherman, D. R.; Boshoff, H. I.; Mizrahi, V. *Chem. Biol.* **2012**, *19*, 844−854.
(34) Singh, S. B.; Phillips, J. W.; Wang, J. *Curr. Opin. Drug Discovery Dev.* **2007**, *10*, 160−166.
(35) Payne, D. J.; Gwynn, M. N.; Holmes, D. J.; Pompliano, D. L. *Nat. Rev. Drug Discovery* **2007**, *6*, 29−40.
(36) Guérot-Fleury, A. M.; Frandsen, N.; Straiger, P. *Gene* **1996**, *180*, 57−61.
(37) Gurevitch, V. V. *Methods Enzymol.* **1996**, *275*, 382−397.